

Resolving exciton diffusion in InGaAs quantum wells using micro-photoluminescence mapping with a lateral excitation

This content has been downloaded from IOPscience. Please scroll down to see the full text.

2013 Semicond. Sci. Technol. 28 125004

(<http://iopscience.iop.org/0268-1242/28/12/125004>)

View [the table of contents for this issue](#), or go to the [journal homepage](#) for more

Download details:

IP Address: 159.226.35.118

This content was downloaded on 29/10/2013 at 06:06

Please note that [terms and conditions apply](#).

Resolving exciton diffusion in InGaAs quantum wells using micro-photoluminescence mapping with a lateral excitation

Shuo Cao^{1,2}, Xiaofan Ji^{1,3}, Kangsheng Qiu¹, Yunan Gao¹, Yanhui Zhao¹, Jing Tang¹, Zheng Xu³, Kuijuan Jin¹ and Xiulai Xu¹

¹ Beijing National Laboratory for Condensed Matter Physics, Institute of Physics, Chinese Academy of Sciences, Beijing 100190, People's Republic of China

² School of Physics, Liaoning University, Shenyang, 110036, People's Republic of China

³ Key Laboratory of Luminescence and Optical Information, Ministry of Education, Institute of Optoelectronics Technology, Beijing Jiaotong University, Beijing, 100044, People's Republic of China

E-mail: kjjin@iphy.ac.cn and xlxu@iphy.ac.cn

Received 12 August 2013, in final form 10 September 2013

Published 24 October 2013

Online at stacks.iop.org/SST/28/125004

Abstract

We report a spatially resolved photoluminescence mapping of InGaAs quantum wells. The photoluminescence was collected on top of the quantum well, with a HeNe laser pumping horizontally or vertically. In the horizontal configuration, at temperature of 68 K, the spectral linewidth narrows from 2.8 to 2.2 meV with the peak shifting from 1.4425 to 1.4415 eV, while at 3.8 K these changes were not observed. This demonstrates that photo-generated carriers can diffuse away from the laser spot and relax to the lower energy states in the case when the charge carriers are thermally activated. The spectra narrowing in the vertical configuration, which could not be observed, is due to the fact that the emitted light was always collected from the same spot of the pumping laser without diffusion.

(Some figures may appear in colour only in the online journal)

1. Introduction

Excitons in a semiconductor have been considered a promising candidate for Bose–Einstein condensation (BEC) [1–4], which brings the quantum effects to a macroscopic scale. In particular, exciton condensation has been demonstrated at a temperature up to 19 K in two-dimensional quantum structures, such as coupled quantum wells [5–7] or quantum wells in optical cavities [8, 9]. The exciton–polariton condensation in nitride-based semiconductor systems could occur at room temperature [10]. However, more convincing evidences for observing the excitonic BEC in semiconductors are still desirable. Recently, the indirect excitons between two coupled quantum wells demonstrated a long-range coherent transport with a distance from a few hundreds of micrometers up to 1 mm [7, 11–15]. However, the mechanism for this long-distance coherent transport is still under debate,

although several mechanisms have been proposed [16–18]. Therefore, understanding the exciton relaxation and diffusion mechanisms in quantum wells is still in demand and challenging.

Spatially and temporally resolved photoluminescence (PL) spectroscopy has been widely used to investigate the exciton distribution in nanostructures [19–23]. Yayan *et al* [20] observed a long-range ($\sim 3 \mu\text{m}$) spatial correlations of the exciton energy distribution using scanning near-field optical microscopy. However, large-scale mapping of quantum wells has not been reported yet, which would be helpful to understand the diffusion process. In this work, we report a spatially resolved PL mapping of InGaAs quantum wells using confocal micro-PL spectroscopy. When the sample was excited laterally with a temperature at 68 K, we observed that the linewidth of the PL spectra decreases as the peak position in energy decreases. However, these changes were

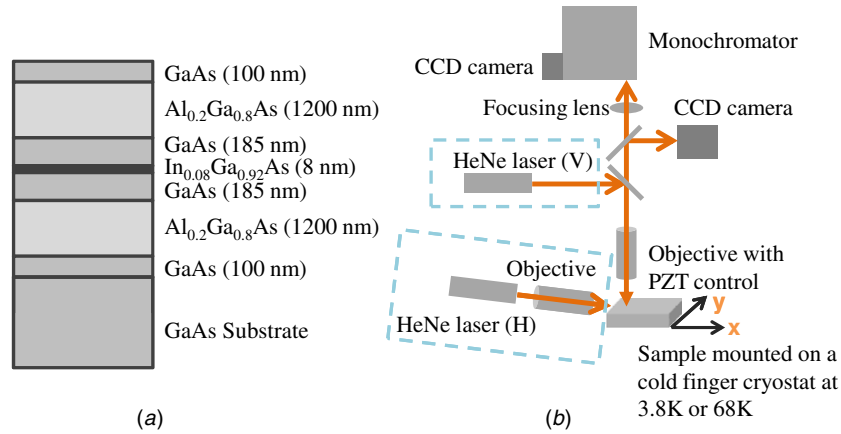


Figure 1. (a) A schematic sketch of the InGaAs quantum well structure. (b) Optical setup for micro-PL mapping with pumping laser exciting from the top (vertical configuration) or from the side (horizontal configuration) of the wafer. The microscopy objective was mounted on an xy piezoelectric stage to perform the PL mapping.

not observed at 3.8 K. This demonstrates that photo-generated carriers can diffuse away from the laser spot and relax to the lower energy states in the case when the charge carriers are thermally activated.

2. Sample structure and experimental details

The structure of the quantum well is shown in figure 1(a). A layer of the In_{0.08}Ga_{0.92}As quantum well with a thickness of 8 nm was sandwiched within a waveguide structure, which was grown by molecular beam epitaxy on a [1 0 0]-oriented undoped GaAs substrate. The layer thicknesses of the structure are labeled in the figure. The PL mapping was performed using a confocal micro-PL setup, as shown in figure 1(b). A HeNe laser was used to excite the quantum well vertically or horizontally. For the vertical configuration, the pump laser light was focused in the vertical direction using a 100 \times microscope objective, with a spot size of 1–2 μm in diameter. The objective was mounted on an xy piezoelectric stage with 100 μm travel along each axis and 1 nm resolution. The PL mapping was carried out by moving the objective position over the quantum well surface. In a single mapping, 41 \times 41 PL spectra were collected within an area of 100 \times 100 μm^2 with a step of 2.5 μm along each axis. The emitted light from the quantum well was collected with the same objective and dispersed through a 0.55 m monochromator, then detected with a liquid-nitrogen-cooled charge-coupled device camera. In the horizontal configuration (figure 1(b)), the pump light excited the sample from the side with a small angle (less than 5 $^\circ$) to the surface using a 20 \times microscope objective. To achieve the mapping area of 100 \times 100 μm^2 , the pumping light was defocused deliberately. The emitted light was collected from the top using the same optical path as mentioned above. The devices were mounted in a He-flow cryostat and cooled to 3.8 K or 68 K using liquid helium or liquid nitrogen, respectively. Due to the working distance (\sim 12 mm) limitation of the objectives, the cryostat was specially designed, which allows us to focus the light on the sample from both directions at low temperature.

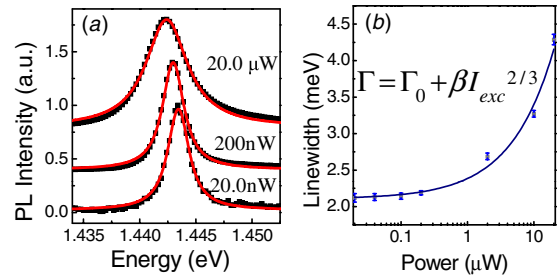


Figure 2. (a) Normalized PL spectra under vertical configuration with different excitation intensities at 68 K. The red solid lines are fitted spectra with a Lorentzian line shape. The lines are vertically shifted for clarity. (b) The measured linewidth as a function of the excitation power. The blue solid line is a fitted curve using the function as shown in the inset.

3. Results and discussion

Figure 2(a) shows the PL spectra with different pumping power in the vertical configuration. It can be seen that the peak position is red shifted slightly when the pumping power increases from 20 nW to 20 μW , which might be due to the local heating effect. The red lines show the fitting results using a Lorentzian function. With the fitting, the PL peak energies, integrated PL intensities and linewidths of the spectra are extracted and discussed throughout this paper. It should be noted that the error bars are different for each spectrum with different pump powers (as shown in figure 2(b)). At a low pumping power of \sim 20 nW, the PL spectra are noisy, resulting in a large error bar for the Lorentzian fit. The error bar then decreases when the spectra are getting smoother. With increasing pumping power over 2 μW , the spectra become asymmetric with a tail at the high-energy side [24], resulting in an increase in the error bar again. The asymmetric spectrum with a tail towards high-energy side indicates a gradual filling effect due to the high excitation density [25]. The generated carrier density with a pumping power at 20 μW is around $1.43 \times 10^{12} \text{ cm}^{-2}$, calculated with a laser spot size of 2 μm in diameter and a reflectance from the surface of 30%. The

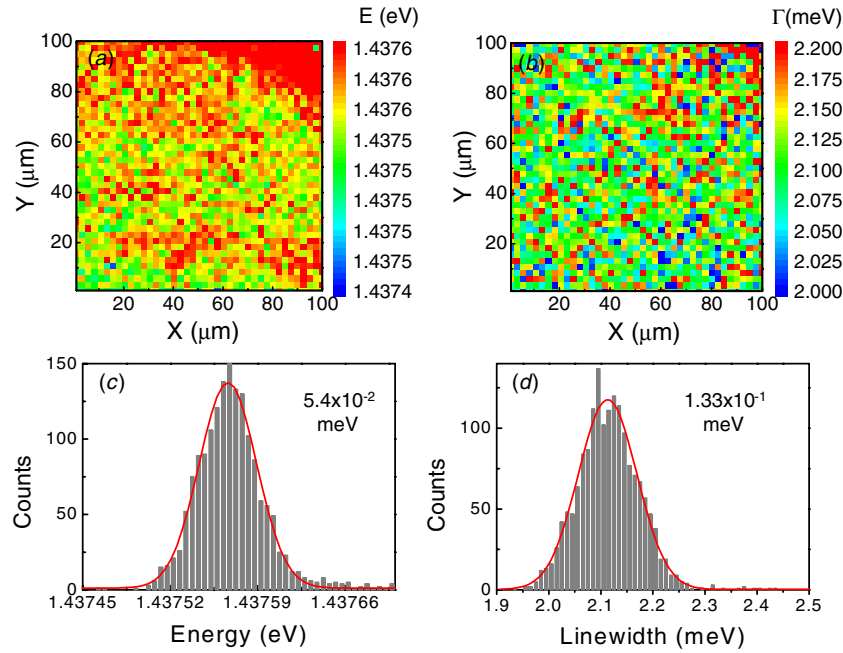


Figure 3. (a) and (b) Peak energy and linewidth mapping in vertical configuration with an excitation power of 20 nW. The sample temperature was at 68 K. The scanning area is about $100 \times 100 \mu\text{m}^2$ with a step of $2.5 \mu\text{m}$ along each axis; 1681 points were collected in total. (c) and (d) The frequency histograms of the peak energy and the linewidth distributions. The red lines are fitted results with the Gaussian function. The values of FWHM are inset in the figures.

linewidths of PL spectra broaden from 2.2 to 4.2 meV with an increase of excitation intensity, as shown in figure 2(b). The linewidth (Γ) as a function of excitation power can be fitted by a power-law dependence [26], $\Gamma = \Gamma_0 + \beta \times I_{\text{exc}}^{2/3}$, where Γ_0 is the limit of Γ at low excitation intensities. The fitting result (the solid blue line) is shown in figure 2(b) with $\Gamma_0 = 2.11$ meV and $\beta = 0.95 \times 10^{-4}$ as the fitting parameters.

Figures 3(a) and (b) show the PL peak position and linewidth mapping in the vertical configuration at 68 K, each of which includes 41×41 scanning points in an area of $100 \times 100 \mu\text{m}^2$. The excitation power was kept at 20 nW. It can be seen that the peak positions and linewidths show a very good uniformity within the mapping area and no correlations can be observed. The histograms of the peak position and the linewidth (as shown in figures 3(c) and (d)) can be fitted nicely using the Gaussian function. The values of the full-width at half-maximum (FWHM) of the histograms are about 5.40×10^{-2} meV and 1.33×10^{-1} meV, respectively.

Similar mapping measurements were performed in the horizontal configuration at 68 K. Figures 4(a), (b) and (c) show the peak position, linewidth and PL intensity mapping of the quantum well with a pumping power of $180 \mu\text{W}$, respectively. The pumping power was measured with a detector after the objective in the optical path, but the absorption by the quantum well was difficult to calibrate precisely in this configuration. Therefore, we cannot compare the pumping power in the two configurations. Figures 4(a) and (b) show that the linewidths strongly correlate with the peak positions, but not with PL intensities as shown in figure 4(c). The correlation can be clearly revealed if we plot the linewidth as a function of the peak energy. Figures 4(d) and (e) show the linewidth as a function of peak energy with pumping power at $180 \mu\text{W}$

and $780 \mu\text{W}$, respectively. The linewidth decreases from 2.8 to 2.2 meV, while the peak energy decreases from 1.4425 to 1.4415 eV. This correlation is independent of excitation intensities within this power range. Normally, the PL linewidth broadening is due to the interface disorders of the quantum wells, which can be modified by varying the quantum well width. For a quantum well with a width larger than 5 nm, the linewidth reduces when the width increases by few nanometers [27]. However, this linewidth narrowing in the same quantum well here can not be simply ascribed to the reduced interface disorder for the quantum well.

In the two configurations, we observed a remarkable difference in the correlation of peak position and the linewidth. We attribute this difference to the effects resulted from photo-generated carriers diffusing and relaxing in the low-energy sites of the energy disorder of the quantum well, which is introduced by the interface disorders or alloy disorders in the quantum well [28, 29]. As there is energy disorder, the carriers preferably occupy the lower energy sites after the diffusion and relaxation. The diffusion length is defined by $\sqrt{D \times \tau}$, where D is the exciton diffusion constant which is around $0.2\text{--}10 \text{ cm}^2 \text{ s}^{-1}$ [30], and τ is the exciton lifetime which is about 1 ns in InGaAs quantum wells. With these parameters, we can calculate the diffusion length is about 140–1000 nm, which can be easily resolved with confocal micro-PL systems using a piezoelectric controlled objective [22, 31, 32]. In the vertical configuration, the PL was collected always at the same point as the pumping laser spot, while in the horizontal configuration, the pump was fixed and the collecting was mapped over the area. Hence, in the first case, the effect of carrier diffusion does not play an important role in the collected PL, but in the latter case most light was collected away from

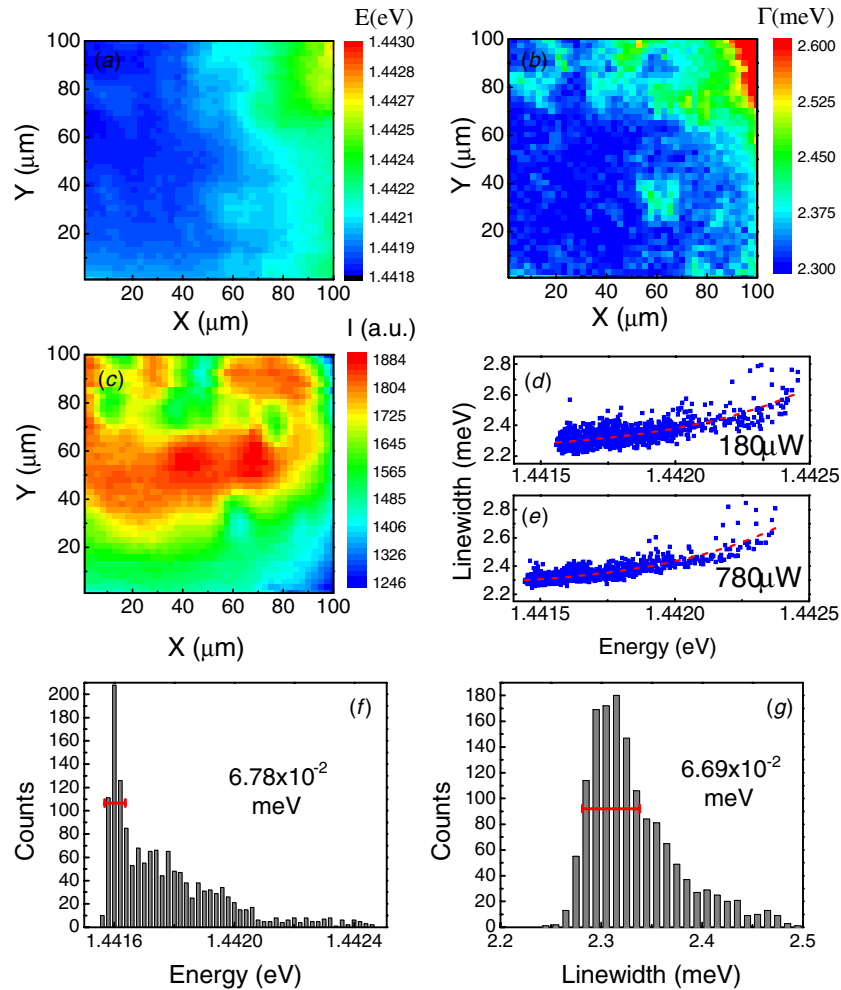


Figure 4. (a)–(c) The peak energy, linewidth and integrated PL intensity mapping (horizontal configuration, 68 K) with an excitation power of $180 \mu\text{W}$. The linewidth as a function of the peak energy with excitation power of $180 \mu\text{W}$ (d) and $780 \mu\text{W}$ (e). The red dashed lines are used to guide the eyes. (f) and (g) The frequency histograms of the emission energy and the linewidth distributions with a pump power of $180 \mu\text{W}$. The values of the peak width marked with the red bars are inset in the figures.

the laser spot which must be due to the diffused excitons. This is further supported by comparing the histograms of the peak position and the line width in figures 3 and 4. In contrast to the Gaussian distribution in figures 3(c) and (d), both peak position and linewidth in figures 4(f) and (g) have a strong peak at low-energy side and a tail towards the high-energy edge. This clearly shows that the carrier is diffused and localized in the lower energy sites, resulting in an asymmetric count distribution. The width of the peak distribution in figure 4(f) (as marked with a red bar) is around $6.78 \times 10^{-2} \text{ meV}$, which is similar to that in figure 3(c). However, the width of the linewidth distribution at $6.69 \times 10^{-2} \text{ meV}$ is only half of that in the vertical configuration, indicating a narrowed linewidth distribution.

One possible reason for the red-shift of the spectra is due to the heating effect by the fluctuation of the pumping laser power during the mapping. However, this can be easily eliminated with the following reasons. The laser power was reduced to a minimum value as long as the PL can be detected, which avoids the heating of the sample. In addition, two PL spectra with peak energy at two extreme cases are normalized and

plotted in figure 5(a). The left edge of the red-shifted spectrum (blue square) does not pass that of the spectrum (the red circle). This confirms that the red-shift is not due to the local heating, because the heating induced red-shift shifts the whole spectrum and even broaden the spectrum. More importantly, this proves our explanation that the diffused carriers preferably occupy the lower energy sites within the quantum well, resulting in a narrowed spectrum within all possible energy states induced by inhomogeneous broadening.

This explanation can be further confirmed by carrying our experiments at a low temperature of 3.8 K. After the excitations, the diffusion process in the energy disorder of the quantum well could only occur when the carriers have enough energy to overcome the energy barriers between energy valleys, as sketched in figure 5(b). At the temperature of 68 K, the thermal energy ($k_B T$) is about 5.85 meV, which is much larger than the energy fluctuation induced linewidth (2.9 meV). While at the temperature of 3.8 K, the thermal energy is only of 0.33 meV, which suggests that there is no carrier diffusion occurring and so there is no correlation between the linewidth and the peak position. Figure 5(c) shows the

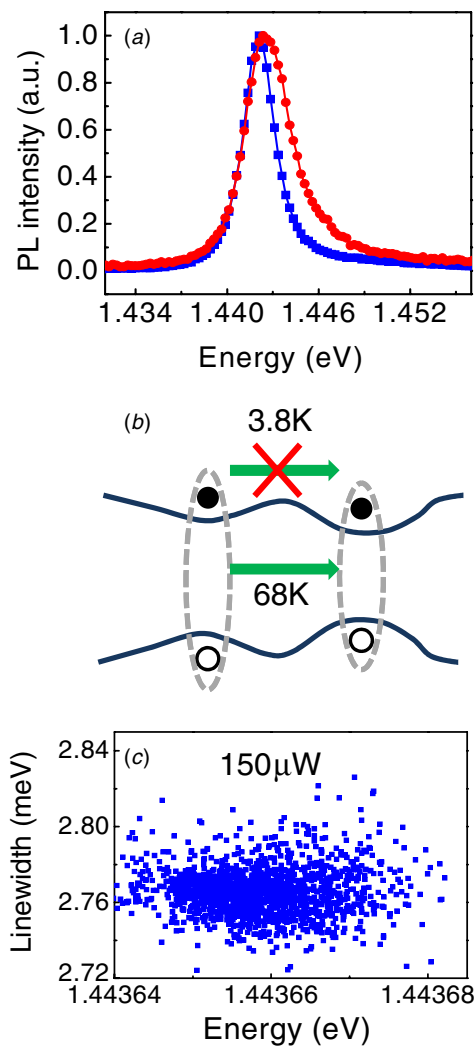


Figure 5. (a) Normalized PL spectra of two extreme cases in the PL mapping in figure 4(a). (b) Schematic sketch of the energy fluctuation of quantum well induces by interface disorders and alloy disorders. The weakly localized carriers at 68 K can be activated and diffuse to the lower energy states, but not at 3.8 K. (c) Linewidth distribution as a function of energy with an excitation power of 150 μW at 3.8 K.

linewidth distribution as a function of the peak position with pump intensities at 150 μW . Indeed, we cannot identify any correlation between the linewidth and the peak position.

4. Conclusion

In summary, PL spectra of the InGaAs quantum well have been mapped with a confocal micro-PL arrangement using both vertical and horizontal configurations. Under the vertical configuration, the linewidth increases with increasing pump power, which is due to the band-filling effect. At the horizontal configuration, the linewidth decreases from 2.8 to 2.2 meV, while the peak position decreases from 1.4425 to 1.4415 eV. In contrast to the results at 3.8 K, we demonstrated that the optically generated carriers at 68 K diffused and relaxed to the lower energy side within the energy states in a single quantum well, resulting in a PL with narrowed linewidth towards the low-energy edge.

Acknowledgments

This work was supported by the National Basic Research Program of China under grant nos 2013CB328 706 and 2012CB921403; the National Natural Science Foundation of China under grant nos 11 174 356, 61 275 060 and 11 134 012; and the Hundred Talents Program of the Chinese Academy of Sciences. ZX was supported by the 973 Program (2010CB327 704), NSFC (51 272 022), NCET (NCET-10-0220), RFDP (20 120 009 130 005) and FRFCU (2012JBZ001).

References

- [1] Hulin D, Mysyrowicz A and Benoit à la Guillaume C 1980 *Phys. Rev. Lett.* **45** 1970
- [2] Lai C W, Zoch J, Gossard A C and Chemla D S 2004 *Science* **303** 503
- [3] Yoshioka K, Chae E and Kuwata-Gonokami M 2011 *Nature Commun.* **2** 328
- [4] Ivanov A L, Littlewood P B and Haug H 1999 *Phys. Rev. B* **59** 5032
- [5] Yang S, Hammack A T, Fogler M M, Butov L V and Gossard A C 2006 *Phys. Rev. Lett.* **97** 187402
- [6] Butov L V, Imamoglu A, Mintsev A V, Campman K L and Gossard A C 1999 *Phys. Rev. B* **59** 1625
- [7] Butov L V, Gossard A C and Chemla D S 2002 *Nature* **418** 751
- [8] Deng H, Weihs G, Santori C, Bloch J and Yamamoto Y 2002 *Science* **298** 199
- [9] Kasprzak J *et al* 2006 *Nature* **443** 409
- [10] Baumberg J J *et al* 2008 *Phys. Rev. Lett.* **101** 136409
- [11] Yang S, Butov L V, Levitov L S, Simons B D and Gossard A C 2010 *Phys. Rev. B* **81** 115320
- [12] Snoke D, Denev S, Liu Y, Pfeiffer L and West K 2002 *Nature* **418** 754
- [13] Fluegel B, Alberi K, Bhusal L, Mascarenhas A, Snoke D W, Karunasiri G, Pfeiffer L N and West K 2011 *Phys. Rev. B* **83** 195320
- [14] Schinner G J, Schubert E, Stallhofer M P, Kotthaus J P, Schuh D, Rai A K, Reuter D, Wieck A D and Govorov A O 2011 *Phys. Rev. B* **83** 165308
- [15] Schinner G J, Repp J, Schubert E, Rai A K, Reuter D, Wieck A D, Govorov A O, Holleitner A W and Kotthaus J P 2013 *Phys. Rev. Lett.* **110** 127403
- [16] Butov L V, Levitov L S, Mintsev A V, Simons B D, Gossard A C and Chemla D S 2004 *Phys. Rev. Lett.* **92** 117404
- [17] Paraskevov A V and Savel'ev S E 2010 *Phys. Rev. B* **81** 193403
- [18] Andreev S V 2013 *Phys. Rev. Lett.* **110** 146401
- [19] Heller W, Filoramo A, Roussignol P and Bockelmann U 1996 *Solid-State Electron.* **40** 725
- [20] Yayon Y, Esser A, Rappaport M, Umansky V, Shtrikman H and Bar-Joseph I 2002 *Phys. Rev. Lett.* **89** 157402
- [21] Yang G, Bolotnikov A E, Cui Y, Camarda G S, Hossain A, Kim K H, Gul R and James R B 2011 *Appl. Phys. Lett.* **98** 261901
- [22] Xu X L, Brossard F S F, Williams D A, Collins D P, Holmes M J, Taylor R A and Zhang X 2010 *New J. Phys.* **12** 083052
- [23] Xu X L, Brossard F S F, Williams D A, Collins D P, Holmes M J, Taylor R A and Zhang X 2009 *Appl. Phys. Lett.* **94** 231103
- [24] Li Z, Wu J, Wang Z M, Fan D, Guo A, Li S, Yu S-Q, Manasreh O and Salamo G J 2010 *Nanoscale Res. Lett.* **5** 1079

- [25] Buyanova I A, Chen W M, Pozina G, Bergman J P, Monemar B, Xin H P and Tu C W 1999 *Appl. Phys. Lett.* **75** 501
- [26] Saucy T, Holtz M, Brafman O, Fekete D and Finkelstein Y 1999 *Phys. Rev. B* **59** 5049
- [27] Patanè A, Polimeni A, Capizzi M and Martelli F 1995 *Phys. Rev. B* **52** 2784
- [28] Singh J and Bajaj K K 1984 *Appl. Phys. Lett.* **44** 1075
- [29] Chen Y, Kothiyal G P, Singh J and Bhattacharya P K 1987 *Superlattices Microstruct.* **3** 657
- [30] Vörös Z, Balili R, Snoke D W, Pfeiffer L and West K 2005 *Phys. Rev. Lett.* **94** 226401
- [31] Zhao H, Dal Don B, Moehl S, Kalt H, Ohkawa K and Hommel D 2003 *Phys. Rev. B* **67** 035306
- [32] Xu X L, Williams D A and Cleaver J R A 2005 *Appl. Phys. Lett.* **86** 012103